

Multiple-stage ambiguity in motion perception reveals global computation of local motion directions

Andrew T. Rider

CoMPLEX, University College London, London, UK
Institute of Ophthalmology, University College London,
London, UK



Shin'ya Nishida

NTT Communication Science Laboratories,
Nippon Telegraph and Telephone Corporation,
Atsugi, Japan



Alan Johnston

CoMPLEX, University College London, London, UK
Experimental Psychology, University College London,
London, UK
School of Psychology, University of Nottingham,
Nottingham, UK



The motion of a 1D image feature, such as a line, seen through a small aperture, or the small receptive field of a neural motion sensor, is underconstrained, and it is not possible to derive the true motion direction from a single local measurement. This is referred to as the aperture problem. How the visual system solves the aperture problem is a fundamental question in visual motion research. In the estimation of motion vectors through integration of ambiguous local motion measurements at different positions, conventional theories assume that the object motion is a rigid translation, with motion signals sharing a common motion vector within the spatial region over which the aperture problem is solved. However, this strategy fails for global rotation. Here we show that the human visual system can estimate global rotation directly through spatial pooling of locally ambiguous measurements, without an intervening step that computes local motion vectors. We designed a novel ambiguous global flow stimulus, which is globally as well as locally ambiguous. The global ambiguity implies that the stimulus is simultaneously consistent with both a global rigid translation and an infinite number of global rigid rotations. By the standard view, the motion should always be seen as a global translation, but it appears to shift from translation to rotation as observers shift fixation. This finding indicates that the visual system can estimate local vectors using a global rotation constraint, and suggests that local motion ambiguity may not be resolved until consistencies with multiple global motion patterns are assessed.

Introduction

The processing of complex visual motion flows by the visual system is generally assumed to follow three consecutive stages (Bradley & Goyal, 2008; Duffy, 2003; Krekelberg, 2008; Pack & Born, 2008). Stage 1: The parallel extraction of local motion signals over the visual field by motion sensors with small receptive fields that consequently suffer from the well-known aperture problem (Wallach, 1935); Stage 2: Integration of ambiguous motion signals into unambiguous 2D velocity signals to solve the aperture problem; and Stage 3: Analysis of the distribution of explicit 2D motion vectors over visual space to extract higher order motion components such as rotation and expansion. Neurophysiological evidence suggests that computation of each stage may take place mainly in V1, MT, and MST, respectively (Graziano, Andersen, & Snowden, 1994). This study challenges the critical computational assumption of this three-stage model: that the aperture problem is solved in Stage 2 before the computation of the complex motion flow in Stage 3.

The aperture problem is caused by the ambiguity of local motion measurements. The motion of a 1D image feature, such as a line, seen through a small aperture, or the small receptive field of a neural motion sensor, is underconstrained, and it is not possible to derive the true motion direction. For a large object, seen through a distributed set of apertures, local contours orthogonal to

Citation: Rider, A. T., Nishida, S., & Johnston, A. (2016). Multiple-stage ambiguity in motion perception reveals global computation of local motion directions. *Journal of Vision*, 16(15):7, 1–11, doi:10.1167/16.15.7.

doi: 10.1167/16.15.7

Received July 5, 2016; published December 9, 2016

ISSN 1534-7362



This work is licensed under a Creative Commons Attribution 4.0 International License.

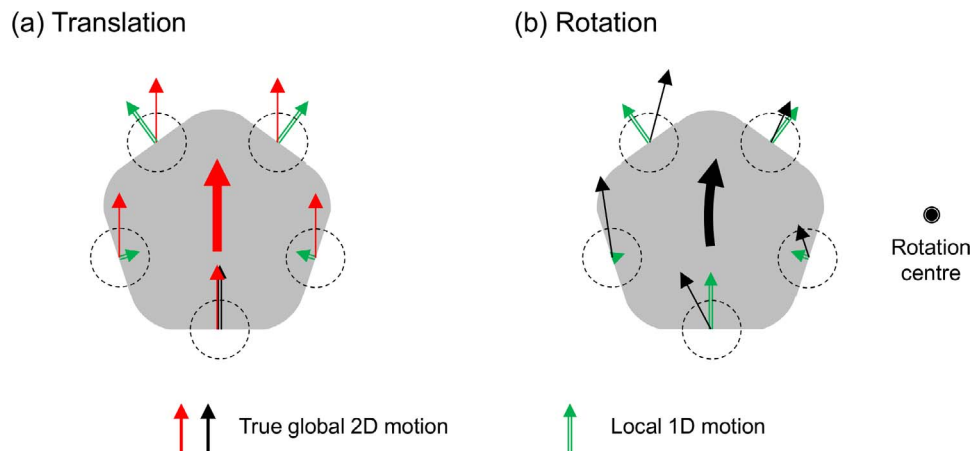


Figure 1. The true 2D motion vector is common across different local motion measurements for translation (a), while it changes in a characteristic way for rotation (b). The visual system has to take into account this difference when integrating ambiguous local motion measurements in order to correctly resolve the aperture problem.

the global motion may convey the correct global motion, but local contours parallel to the global motion slide along themselves and consequently, the orthogonal (normal) component of motion is zero (Hildreth, 1984). For a solution of the aperture problem, these disparate and spatially distributed local ambiguous estimates need to be brought together in a way that delivers the correct motion vector at each point on the object (Figure 1a). The prevailing view is that visual system resolves the aperture problem by combining multiple ambiguous local measurements through an intersection of constraints (Adelson & Movshon, 1982; Weiss, Simoncelli, & Adelson, 2002), vector average (Wilson & Kim, 1994) or harmonic vector average (Johnston & Scarfe, 2013) algorithm. Despite the difference in the combination rule, these algorithms are based on a common assumption, that the integrated local motion measurements share the same unique global motion vector. This “rigidity” assumption is unquestionably valid for integration of motion signals sampled at the same location. For spatially distributed motion measurements, however, a common vector is a too strong, and often incorrect, assumption in a natural scene.

The natural optic flow produced on the retina by the movements of objects or the observer has several unique patterns that the visual system may use to resolve the motion ambiguity. According to Koenderink (1986), the motion flow can in general be decomposed into four components: translation, divergence, deformation, and curl (the mathematical descriptor of rotation). Due to perspective projection, movements of a rigid object in the three-dimensional space produces complex optic flows including divergence and deformation components. Even when only the movement of a rigid object in a frontal parallel plane is considered, the motion flow on the retina often contains a rotation component, in addition to a

translation component. The rotation flow is produced not only by a rotation of the object, but also by the eye/head rotation of an observer, around the viewing axis. For rotation, the global motion solution implies a particular spatial distribution of local velocities, rather than a single global velocity (Figure 1b). A better computation to resolve the aperture problem in this case is to assume a rigid rotation in addition to a rigid translation than to assume a rigid translation alone, in interpreting the ambiguous motion measurements. Whether the visual system implements such an elegant, but complicated, computation has not been tested. Rather, based on the three-stage model, it has typically been thought that complex optic flows including global rotation are processed in Stage 3 after local motion measurement ambiguity is resolved in Stage 2 with the assumption that the object motion is spatially smooth (Hildreth, 1984; Weiss et al., 2002), or approximately a rigid translation at least within the spatial neighborhood over which the aperture problem is solved.

Here we report a novel ambiguous global flow pattern (which, according to the standard view, should always be seen as global translation regardless of the size of integration window) appears to shift from translation to rotation as observers shift fixation. This indicates that the visual system can estimate local vectors using a global rotation constraint, and suggests that local motion ambiguity is not resolved until consistencies with multiple complex motions are assessed.

Ambiguous motion stimuli

We made a motion display consisting of multiple ambiguous motion elements that is simultaneously

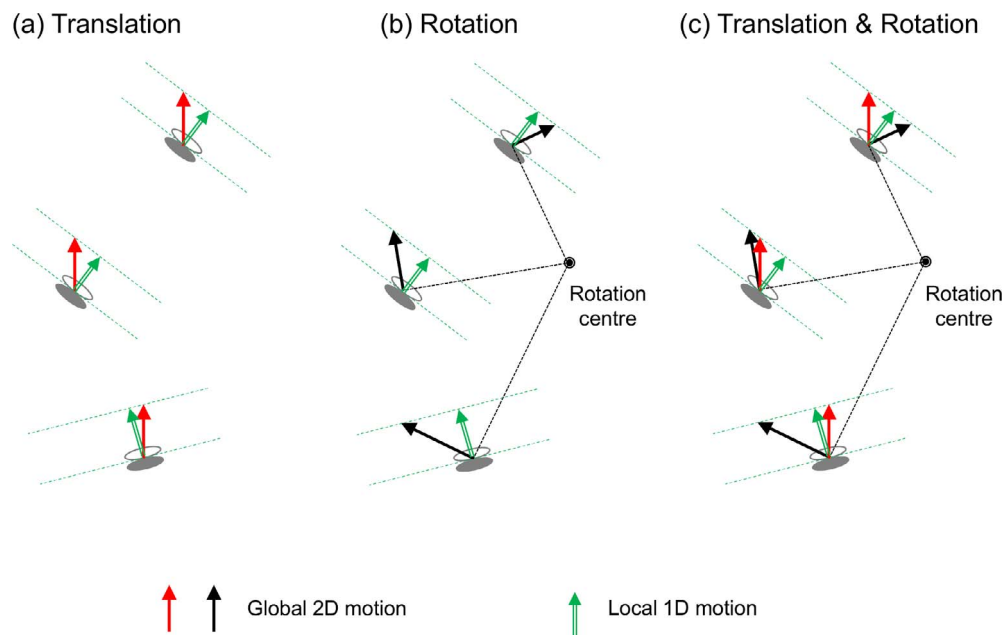


Figure 2. (a) How to make the movement of multiple Gabor patches consistent with a global translation. Blue arrows indicate the true motion vectors of the optic flow, which are common across patches. The orientation of each Gabor can be arbitrarily determined, and the drifting speed of each Gabor is the true vector component projected to the normal direction of the Gabor orientation. (b) How to make the movement of multiple Gabor patches consistent with a global rotation around a single point. Red arrows indicate the true motion vectors of the optic flow, which changes depending on the patch location. Again, the orientation of each Gabor can be arbitrarily determined, and the drifting speed of each Gabor is the true vector component projected to the normal direction of the Gabor orientation. (c) How to make the movement of multiple Gabor patches consistent with a global translation and a global rotation. Now at each location, there are two true vectors (red and black arrows). To make Gabor motion consistent with both of them, the Gabor orientation is set parallel to the line connecting to the end points of the two vectors. Then for the two true vectors, the component projected to the normal direction of the Gabor orientation becomes identical, as indicated by green arrows.

compatible with a global translation and a global rotation. It consisted of multiple one-dimensional motion elements (Amano, Edwards, Badcock, & Nishida, 2009; Lorenceau & Alais, 2001; Lorenceau & Shiffrar, 1992; Lorenceau & Zago, 1999; Mingolla, Todd, & Norman, 1992; Rider, McOwan, & Johnston, 2014; Rubin, Hochstein, & Solomon, 1995; Takeuchi, 1998). Each element was a dynamic Gabor: a drifting sinewave with a stationary Gaussian envelope (Amano et al., 2009). With Gabor motion arrays, the true motion direction can be estimated from an integration of 1D motion signals from at least two Gabors having different orientations (Adelson & Movshon, 1982). It cannot be estimated from the movements of 2D features such as line terminations and corners (Pack, Livingstone, Duffy, & Born, 2003). In a standard global Gabor array, giving rise to the perception of a global translation, or to the perception of a global rotation, once a global velocity is set, the local orientation of the Gabor can be chosen at random, with the local speed determined by the true 2D motion vector at the location and by the choice of local orientation (Amano et al., 2009; Figures 2a and b). This leaves us one degree of freedom in designing a globally ambiguous array. By setting the orientation and speed

of each Gabor motion to be consistent with two 2D vectors at each location, it is possible to make a Gabor array simultaneously consistent with a global translation and a single global rotation (Figure 2c). Furthermore, this pattern of local motion is also consistent with rotation around any point that lies on a horizontal line through the origin of the array (see Appendix A for the mathematical proof). That is, the pattern is consistent with a fast angular rotation about a near point and a slow angular rotation about a far point. For an infinitely far rotation point, the motion patterns for the putative linear translation and rotation are identical. The global motion remains ambiguous regardless of the size of motion pooling window.

When we set the direction of global translation upward or downward, the resulting ambiguous motion array is circularly symmetric in orientation, and vertically symmetric in direction. In our stimulus presentation, we used a circular region in which all the elements orient along concentric circles (Figure 3 left and Supplementary Movie 1); note that the central region was removed as it has been shown that global motion perception is much weaker in the fovea (Takeuchi, 1998). The reason for this symmetrical arrangement was to exclude any possible bias caused by

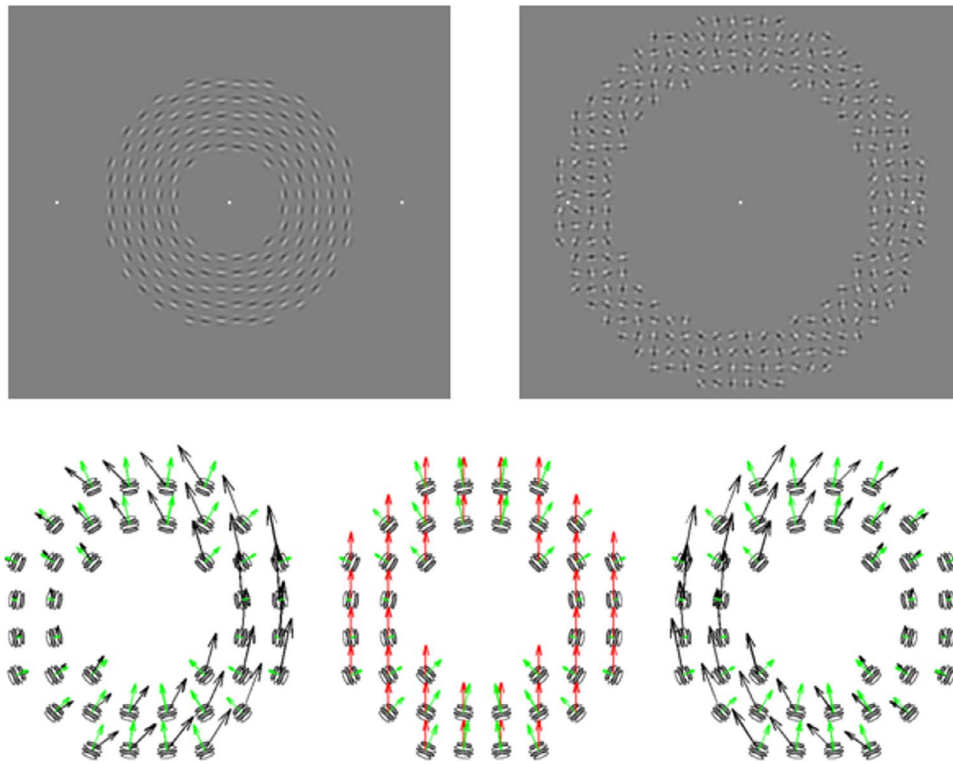


Figure 3. The design of the ambiguous array. Top left: the multi-ambiguous Gabor array. White dots indicate fixation points; only one was shown during any given trial. Top right: the flanking plaid array; note that the Gabor array and plaid array were not on screen simultaneously at any point. Bottom: global and local motions for three global solutions including a translation (centre) and two rotations. Local motions are shown in green and are identical for all three patterns. Underlying global motion solutions are shown in black for rotation and red for translation.

an asymmetric stimulus arrangement, i.e., a mechanism which extracts either a vector average or the intersection of constraints would signal the same vertical direction. It should be noted that the rotation around the center of the annular region, which one might expect with this type of configuration, is not included in the set of rotations consistent with the Gabor array (it is a limiting case which is not explicitly included in the set of solutions; see Appendix A).

If the visual system only uses the common vector assumption to solve the aperture problem, as the standard theories predict, the stimulus should be seen as a global upward translation. On the other hand, if the visual system uses rotation as an additional constraint to solve the aperture problem, the stimulus might be seen as a global rotation under some conditions. Our preliminary observation suggests that a global upward translation is seen when observers look directly at the stimulus. However, when they view the same stimulus in the periphery, they see rotation, the center of which changes as the observers shift fixation (see Supplementary Movie 1).

The following experiments confirmed this observation, and showed that this gaze-dependent motion ambiguity is a unique feature of this stimulus.

Methods

Subjects

Subjects were one of the authors (AR) and three naïve observers who had normal or corrected-to-normal visual acuity.

Stimuli and procedures

To measure the perceived motion of the ambiguous array, we used a motion matching task in which subjects adjusted the motion of a surrounding annulus of (locally unambiguous) plaid patches until they had the same global motion appearance as the Gabor array. This task involved adjusting the speed and center of rotation of the plaid array. Three fixation points were used in different trials: one on either side of the Gabor array and one in the center.

Stimuli were generated using Psychtoolbox and presented on a Mitsubishi Diamond Plus 230SB monitor (1024 × 768 pixels, 100 Hz refresh rate). The viewing distance of 57 cm was maintained using a chinrest.

The ambiguous stimulus array consisted of 176 Gabors arranged on a regular 1.18° by 1.18° grid confined within an annulus covering 3.55° – 9.46° from the center of the screen. The Gabors comprised a sinewave grating, spatial frequency = 0.6 cycles/ $^\circ$, multiplied by a 2D Gaussian, space constant = 0.24° . Contrast was fixed at 30%. The orientations of the Gabors were orthogonal to a radial pattern centered on the middle of the display. The motion of the Gabor array was always consistent with a rigid vertical translation with a speed of 1.18° /s. The direction of vertical translation alternated from trial to trial.

The comparison array consisted of 240 plaid patches presented on the same grid pattern but more peripherally, i.e., within an annulus covering 9.46° – 14.18° . The orientation of one of the plaid components in each patch was chosen at random; the second component was always orthogonal to the first.

The target array and the comparison were spatially and temporally separated with subjects pressing the mouse button to toggle between the two. This should minimize any influence of motion aftereffects or of motion repulsion/assimilation. Plaid motion was set to be consistent with a global motion that depended on two variables: (angular) speed and the position of the center of rotation. Subjects manipulated these variables in real time using a trackball. The horizontal axis controlled the speed, s , according to the relationship $s = 3 \frac{x-h}{h}$ where x is the current horizontal position of the trackball-controlled cursor (from 1 to 1024 pixels) and h is the horizontal midpoint of the screen. This allowed subjects to vary the speed from $1/3$ to 3 times the veridical speed of the array. The exponential relationship between x and s ensures that a shift of a given number of pixels will always produce the same proportional change in speed. This relationship was chosen as speed discrimination has been shown to be consistent with Weber's law, i.e., discrimination threshold is proportional to the absolute speed (Snowden & Braddick, 1991). The vertical axis controlled the curvature of the velocity field by varying the distance, d , of the center of rotation from the center of the display (note the center of rotation was always on the horizontal meridian), i.e.

$$d = \frac{3v}{v-y},$$

where v is the vertical midpoint of the display and y is the current vertical position, measured in Gabor patch sized units (i.e., 1 unit = 1.18 cm). The denominator goes to zero when $v = y$ and in this case the distance to center was set at 10,000 (i.e., a nominal distance of 118 m), which approximates a translation (a translation can be considered to be identical to a rotation about some notional point "at infinity"). Subjects could therefore adjust the speed and curvature of the plaid stimulus,

while freely switching between plaids and Gabors. Subjects viewed the stimulus for as long as they wished; and when they were satisfied the two motions appeared similar, a button press recorded the coordinates of the cursor and initiated the next trial. The cursor was not displayed on screen at any time during the experiment. Three fixation points were used: the center of the display, 13° to the left and 13° to the right of center. These three fixation points were randomly interleaved over trials. There were 120 trials per block (20 repetitions of three fixation conditions for each of two direction conditions: upwards and downwards). No fixed limit was placed on trial duration, but each block lasted approximately 30 minutes.

In control experiments, we used the following three stimuli: (a) a segmented ambiguous array that was constructed in the same way as the full array except that Gabors falling within two 90° arcs centered on the horizontal midline to the right and left of the array were removed; (b) a translational Gabor array that consisted of Gabor elements with random orientations, and the speed of each Gabor was set to be consistent only with a global vertical translation; and (c) a plaid array that consisted of Gabor plaid elements. The orientation of one of the plaid components in each patch was chosen at random; the second component was always orthogonal to the first. The motion of each Gabor plaid simulated the local motion in the normal direction of the ambiguous Gabor array.

Results

We found that subjects perceived three distinct types of global motion depending on the position of fixation relative to the center of the array (furthest left column of Figure 4). Central fixation induced a perception of vertical translation in three out of four subjects (blue symbols). Fixation to the left (red symbols) or right (green symbols) caused the array to appear to rotate with a center approximately at fixation. It is clear that, in the periphery, local motion ambiguity is resolved by the global rotation constraint rather than the global translation constraint.

Our stimulus is ambiguous not only in relation to the type of global motion (translation or rotation), but also with respect to the center of rotation. For the symmetric full array, the perceived rotation was always centered on the fixation point, but off-center rotation could also be a solution. When 90° sections of the array to the left and right of center were removed, stimulus (a), creating a segmented array in which the motions are still consistent with the same set of global solutions as the full array, subjects again perceived rigid translation for central fixation and rotations for peripheral fixations, but

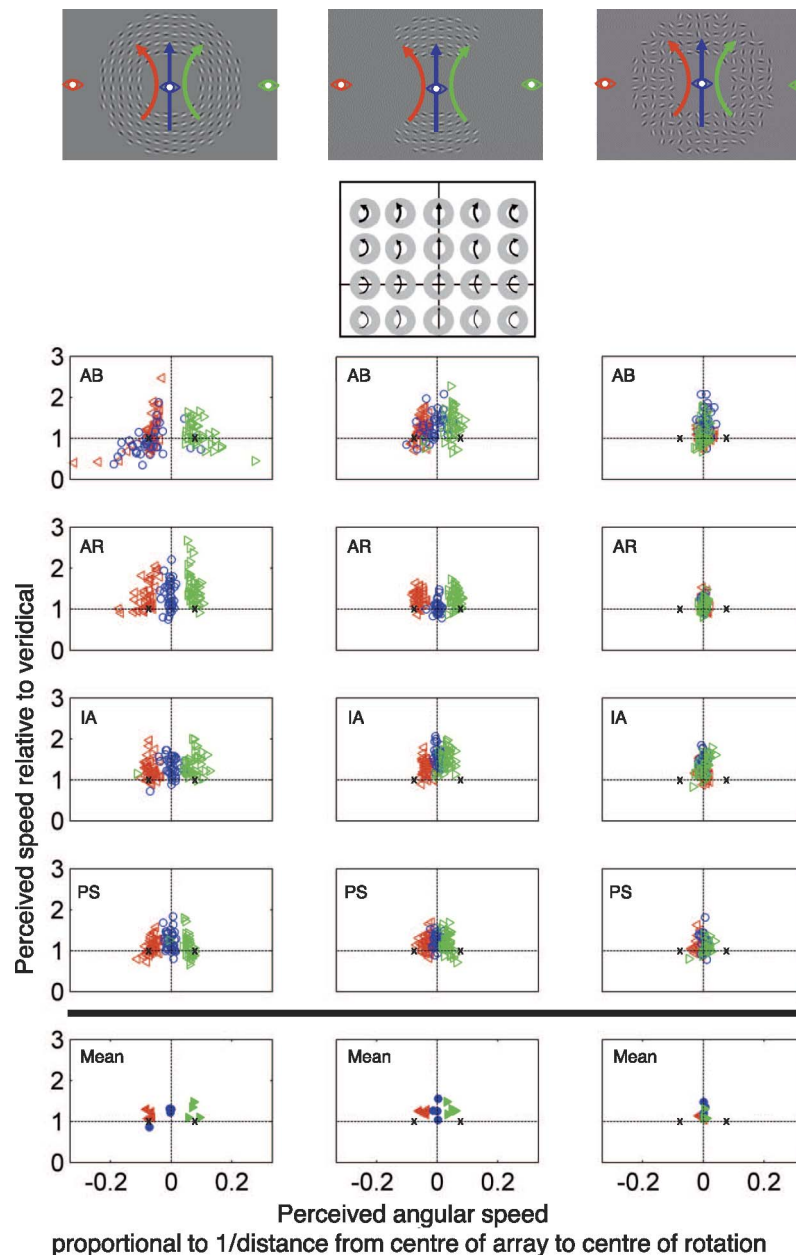


Figure 4. Results of motion-matching experiments. Left column: full array; Centre column: segmented array; and Right column: randomly oriented Gabors. Top: example of test stimulus with red, blue, and green fixation eye symbols denoting the left, center, and right fixation points respectively. Top middle: diagram of motion space used in these graphs; thickness of arrows is proportional to the global speed. Middle: individual results for four subjects; the black x symbols denote rotation around the two eccentric fixation points. Bottom: mean values.

crucially the center of rotation was significantly different from fixation (Figure 4, center column). This finding rules out an explanation based on a simple tendency to perceive rotation about fixation. Why did the perceived motion become closer to the upward translation by removing the left and right segments? This is possibly because spatial interactions leading to a globally coherent percept are disrupted, and the remaining upper and lower segments contain many horizontal elements that tend to appear to move upward unless being otherwise con-

strained by a global factor. It is clear from Figure 3 that the largest differential in local velocity between translation and rotation about fixation is removed in the segmented array (compare the red and black arrows in Figure 3). When the 2D velocities implied by the two global motion types are more similar, it might be that the visual system may find a solution that approximates both.

One may consider that what we found was a general visual eccentricity dependent effect, such as a differential tendency to cohere, regardless of the stimulus. To

test this, we measured global motion perception of Gabor arrays with random orientations, whose carrier motions were consistent with a global translation, stimulus (b). These stimuli always appear to globally translate. They never induced a perception of rotation when viewed peripherally (furthest right column in Figure 4 and Supplementary Movie 2). This indicates that the eccentricity-dependent change in global motion appearance is not a general phenomenon observed with Global Gabor motion arrays.

Furthermore, when the local motion was made unambiguous through the use of local plaid elements displaying the normal component of the ambiguous motion pattern elements, stimulus (c), a noncoherent global motion could be observed which was not altered by changes in fixation (see Supplementary Movie 3). This indicates that when the local motion is unambiguously determined, observers see the local velocity field as specified and do not integrate these local velocities into a single global solution, and, in addition, that the eccentricity-dependent change in global motion is related to the solution of the aperture problem by global constraints. Note that subjects were unable to find a perceptual match to this stimulus among the set of motions available, so no data is presented in Figure 4.

Discussion

We found that the same locally ambiguous motion array can give rise to multiple global motion pattern percepts depending on where in the stimulus the observer looks.

Past studies have found several differences in motion perception between the central and peripheral visual fields (De Bruyn, 1997; Edwards & Nishida, 2004; Hisakata & Murakami, 2008; Johnston & Wright, 1986; Mather, Cavanagh, & Anstis, 1985; Murakami & Shimojo, 1993; Takeuchi, 1998; Tse & Hsieh, 2006; Yo & Wilson, 1992), but these differences have been ascribed to an increase in the spatial scale of motion processing as a function of retinal eccentricity, and/or reduced contributions of form-sensitive mechanisms in the periphery. It is difficult on the basis of these factors to explain why a global translation seen with the central fixation is changed into global rotations for peripheral fixations, since both types of global motion are expected to be enhanced in peripheral vision, and our stimulus was large enough to stimulate peripheral vision even with central fixation. Furthermore, perceived velocity is reduced in the visual periphery (Johnston & Wright, 1986) which would act against the perception of rotation for off-center fixations. In

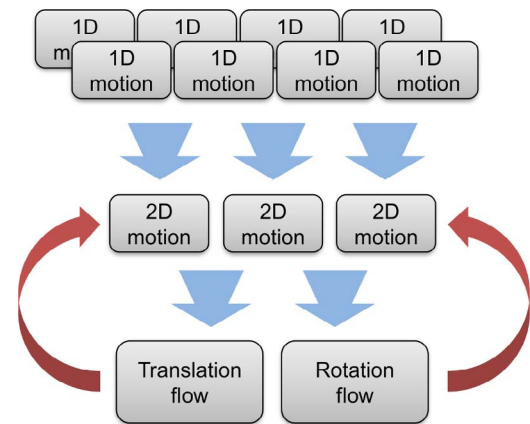


Figure 5. Visual motion processing suggested by the present study. Blue arrows indicate feedforward routes wherein 1D local motion signals are integrated over space, orientation and spatiotemporal frequency to compute 2D motion vectors, which are then spatially pooled to compute motion flow patterns. Red arrows indicate feedback routes through which the consistency with global motion flow affects computation of 2D motion vectors.

addition, our control experiments with unambiguous stimuli ruled out a simple effect of eccentricity.

Our key finding indicates that locally ambiguous motion is not resolved to a single local explicit velocity code on the basis of a local rigid assumption but rather that a number of global motion options are entertained prior to the selection of a single global motion solution and its consequent local motion interpretation (Figure 5). This may be viewed as an extension of “adaptive pooling” (Amano et al., 2009) to cover more complex motion fields such as rotation. The rotation-sensitive mechanism tapped by our stimulus may explain a number of studies which have found a “complexity advantage” in which sensitivity (Freeman & Harris, 1992; Lee & Lu, 2010) or the motion aftereffect (Bex, Metha, & Makous, 1999) is enhanced for rotations relative to translations.

A currently popular computational theory of visual motion integration is a Bayesian model (Weiss & Adelson, 1998; Yuille & Grzywacz, 1988), which assumes that “smooth and slow” priors influence motion integration more strongly in areas of the higher uncertainty (e.g., in the periphery). This model cannot explain our results. A rigid translation is the smoothest possible (i.e., uniform) velocity field so a smoothness prior should not favor rotation over translation when the stimulus is viewed more peripherally, as is the case with our stimulus. Further, it can be shown that for our stimulus the translation solution is, on average, the slowest global solution (see Appendix B). Worse still, subjects tended to see rotation about a point near fixation, in which case the velocity field is slowest near fixation and is fastest in the periphery, so a slowness prior that takes precedence in the “uncertain” periph-

ery is also inconsistent with our findings. Adding a further prior for seeing rotation around fixation may allow their model to predict our results, but it is not clear how these disparate priors would need to be balanced over visual space.

Lorenceau and colleagues (Lorenceau & Alais, 2001; Lorenceau & Shiffrar, 1992; Lorenceau & Zago, 1999) found several influences of form for line segments and gratings, e.g., the presence of “virtual junctions” between differently oriented grating patches, can influence the tendency to see global rotation. Since our ambiguous stimulus has a specific orientation structure, form information might have some influence on motion percepts, but this factor cannot explain why global motion perception changes with fixation.

Whereas the present study suggests a global computation is required to resolve the aperture problem, past neurophysiological studies have suggested local motion integration is accomplished by neurons in MT (Movshon, Adelson, Gizzi, & Newsome, 1985) which is not sensitive to complex motions like rotation (Tanaka et al., 1986). One possible resolution of this discrepancy is that the aperture problem is not resolved by neurons in MT, at least for the type of stimulus we used. In agreement with this possibility, it has been shown that the response of MT neuron is not always correlated with the perceived global motion (Hedges et al., 2011). Also, MT neurons do not respond to pattern motion for “pseudoplaids”—two Gabors spatially separate but still within the cell’s receptive field (Majaj, Carandini, & Movshon, 2007)—but it is worth noting that the sparse stimuli they used do not contain the rich contextual information of a multi-aperture array, such as we use, and would not be perceived as moving coherently. Imaging techniques indicate a selective response for global motion in MT (Amano et al., 2012). Another possibility is that the aperture problem is solved in MT but with the acceptance that the IOC solution (often termed the Pattern Direction) is only one of many possible solutions if we allow the local velocity to vary over space, as occurs with rotation. We note that many (>40%) neurons in MT do not appear to signal either the local (Component Direction) or global (Pattern Direction, i.e., IOC) motion (Majaj et al., 2007; Movshon et al., 1985). The population of candidate solutions to the aperture problem would then be examined by neurons in MST for consistency with global complex flows such as rotation.

Alternatively, MT neurons may represent local motion vectors consistent with the perceived motion flow even for the stimulus we used, since it has been shown that the motion integration performance of MT neurons is dramatically altered by the stimulus context (Huang, Albright, & Stoner, 2008). If this is the case, our finding suggests the influence of feedback from MST, where global complex flow information is

represented. The perception of rotation around fixation may reflect a general preference of the neurons in MST for global image rotations around the fixation point, which are often produced when observers move their head while gazing at a target (Duffy & Wurtz, 1995).

At present, we can only speculate about the neurophysiological implications of our findings. We can however conclude that in order to explain our findings, one needs to update the standard computational view about visual motion processing, and our stimulus will provide a useful tool to analyze this yet to be determined neural network in the future.

Keywords: visual motion perception, aperture problem, optical flow, perceptual ambiguity

Acknowledgments

A.R. was supported by an EPSRC studentship awarded by the CoMPLEX DTC, grant number EP/C512901/1. S.N. was supported by MEXT/JSPS KAKENHI Grant Number JP15H05915. A.J. was supported by the BBSRC (BB/F01354X/1) and the Leverhulme Trust.

Commercial relationships: none.

Corresponding author: Andrew Thomas Rider.

Email: a.rider@ucl.ac.uk.

Address: CoMPLEX, University College London, London, UK; Institute of Ophthalmology, University College London, London, UK.

References

- Adelson, E. H., & Movshon, J. A. (1982). Phenomenal Coherence of Moving Visual-Patterns. *Nature*, *300*(5892), 523–525.
- Amano, K., Edwards, M., Badcock, D. R., & Nishida, S. (2009). Adaptive pooling of visual motion signals by the human visual system revealed with a novel multi-element stimulus. *Journal of vision*, *9*(3):4, 1–25, doi:10.1167/9.3.4. [PubMed] [Article]
- Amano, K., Takeda, T., Haji, T., Terao, M., Maruya, K., Matsumoto, K., & Nishida, S. (2012). Human neural responses involved in spatial pooling of locally ambiguous motion signals. *Journal of Neurophysiology*, *107*(12), 3493–3508, doi:10.1152/jn.00821.2011.
- Bex, P. J., Metha, A. B., & Makous, W. (1999). Enhanced motion aftereffect for complex motions. *Vision Research*, *39*(13), 2229–2238.
- Bradley, D. C., & Goyal, M. S. (2008). Velocity

- computation in the primate visual system. *Nature Reviews Neuroscience*, 9(9), 686–695, doi:10.1038/nrn2472.
- De Bruyn, B. (1997). Blending transparent motion patterns in peripheral vision. *Vision Research*, 37(5), 645–648.
- Duffy, C. J. (2003). The cortical analysis of optical flow. In L. M. Chalupa & J. S. Werner (Eds.), *The visual neurosciences* (Vol. 2., pp. 1260–1283). Cambridge MA: MIT Press.
- Duffy, C. J., & Wurtz, R. H. (1995). Response of monkey MST neurons to optic flow stimuli with shifted centers of motion. *Journal of Neuroscience*, 15(7 Pt. 2), 5192–5208.
- Edwards, M., & Nishida, S. (2004). Contrast-reversing global-motion stimuli reveal local interactions between first- and second-order motion signals. *Vision Research*, 44(16), 1941–1950, doi:10.1016/j.visres.2004.03.016.
- Freeman, T. C. A., & Harris, M. G. (1992). Human sensitivity to expanding and rotating motion: Effects of complementary masking and directional structure. *Vision Research*, 32(1), 81–87.
- Graziano, M. S. A., Andersen, R. A., & Snowden, R. J. (1994). Tuning of MST to spiral motions. *Journal of Neuroscience*, 14, 54–67.
- Hedges, J. H., Gartshteyn, Y., Kohn, A., Rust, N. C., Shadlen, M. N., Newsome, W. T., & Movshon, J. A. (2011). Dissociation of neuronal and psychophysical responses to local and global motion. *Current Biology*, 21(23), 2023–2028, doi:10.1016/j.cub.2011.10.049.
- Hildreth, E. C. (1984). The computation of the velocity-field. *Proceedings of the Royal Society of London Series B: Biological Sciences*, 221(1223), 189–220.
- Hisakata, R., & Murakami, I. (2008). The effects of eccentricity and retinal illuminance on the illusory motion seen in a stationary luminance gradient. *Vision Research*, 48(19), 1940–1948, doi:10.1016/j.visres.2008.06.015.
- Huang, X., Albright, T. D., & Stoner, G. R. (2008). Stimulus dependency and mechanisms of surround modulation in cortical area MT. *Journal of Neuroscience*, 28(51), 13889–13906, doi:10.1523/JNEUROSCI.1946-08.2008.
- Johnston, A., & Scarfe, P. (2013). The role of the harmonic vector average in motion integration. *Frontiers in Computational Neuroscience*, 7, 146, doi:10.3389/fncom.2013.00146.earch
- Johnston, A., & Wright, M. J. (1986). Matching velocity in central and peripheral vision. *Vision Research*, 26, 1099–1109.
- Koenderink, J. J. (1986). Optic flow. *Vision Research*, 26(1), 161–179.
- Krekelberg, B. (2008). Motion detection mechanisms. In A. I. Basbaum, A. Kaneko, G. M. Shepherd, & G. Westheimer (Eds.), *The senses: A comprehensive reference*. (Vol. 2., pp. 133–154). Oxford: Elsevier Inc.
- Lee, A. L. F., & Lu, H. (2010). A comparison of global motion perception using a multiple-aperture stimulus. *Journal of Vision*, 10(4):9, 1–16, doi:10.1167/10.4.9. [PubMed] [Article]
- Lorenceau, J., & Alais, D. (2001). Form constraints in motion binding. *Nature Neuroscience*, 4(7), 745–751.
- Lorenceau, J., & Shiffrar, M. (1992). The influence of terminators on motion integration across space. *Vision Research*, 32(2), 263–273.
- Lorenceau, J., & Zago, L. (1999). Cooperative and competitive spatial interactions in motion integration. *Visual Neuroscience*, 16(4), 755–770.
- Majaj, N. J., Carandini, M., & Movshon, J. A. (2007). Motion integration by neurons in macaque MT is local, not global. *Journal of Neuroscience*, 27(2), 366–370, doi:10.1523/Jneurosci.3183-06.2007.
- Mather, G., Cavanagh, P., & Anstis, S. M. (1985). A moving display which opposes short-range and long-range signals. *Perception*, 14(2), 163–166.
- Mingolla, E., Todd, J. T., Norman, J. F. (1992). The perception of globally coherent motion. *Vision Research*, 32(6), 1015–1031.
- Movshon, J. A., Adelson, E. H., Gizzi, E. H., & Newsome, W. T. (1985). The analysis of moving visual patterns. In C. Chagass, R. Gattas, & C. Gross (Eds.), *Pattern recognition mechanisms* (pp. 117–151). New York: Springer.
- Murakami, I., & Shimojo, S. (1993). Motion capture changes to induced motion at higher luminance contrasts, smaller eccentricities, and larger inducer sizes. *Vision Research*, 33(15), 2091–2107.
- Pack, C., & Born, R. (2008). Cortical mechanisms for the integration of visual motion. In A. I. Basbaum, A. Kaneko, G. M. Shepherd, & G. Westheimer (Eds.), *The senses: A comprehensive reference* (Vol. 2, pp. 189–218). Cambridge, MA: Academic Press.
- Pack, C., Livingstone, M. S., Duffy, K. R., & Born, R. T. (2003). End-stopping and the aperture problem: Two-dimensional motion signals in macaque V1. *Neuron*, 39(4), 671–680.
- Rider, A. T., McOwan, P. W., & Johnston, A. (2014). Asymmetric global motion integration in drifting Gabor arrays. *Journal of Vision*, 14(8):18, 1–10, doi:10.1167/14.8.18. [PubMed] [Article]
- Rubin, N., Hochstein, S., & Solomon, S. (1995). Restricted ability to recover three-dimensional global motion from one-dimensional motion sig-

nals: Psychophysical observations. *Vision Research*, 35(4), 463–476.

Snowden, R. J., & Braddick, O. J. (1991). The temporal integration and resolution of velocity signals. *Vision Research*, 31(5), 907–914.

Takeuchi, T. (1998). Effect of contrast on the perception of moving multiple Gabor patterns. *Vision Research*, 38(20), 3069–3082.

Tanaka, K., Hikosaka, K., Saito, H., Yukie, M., Fukada, Y., & Iwai, E. (1986). Analysis of local and wide-field movements in the superior temporal visual areas of the macaque monkey. *Journal of Neuroscience*, 6(1), 134–144.

Tse, P. U., & Hsieh, P. J. (2006). The infinite regress illusion reveals faulty integration of local and global motion signals. *Vision Research*, 46(22), 3881–3885, doi:10.1016/j.visres.2006.06.010.

Wallach, H. (1935). Ueber visuell wahrgenommene Bewegungsrichtung [Translation: On the visually perceived direction of motion]. *Psychologische Forschung*, 20, 325–380.

Weiss, Y., & Adelson, E. H. (1998). Slow and smooth: A Bayesian theory for the combination of local motion signals in human vision. In *Technical report AI memo 1624*. Cambridge, MA: MIT AI Lab.

Weiss, Y., Simoncelli, E. P., & Adelson, E. H. (2002). Motion illusions as optimal percepts. *Nature Neuroscience*, 5(6), 598–604, doi:10.1038/Nn858.

Wilson, H. R., & Kim, J. (1994). Perceived motion in the vector sum direction. *Vision Research*, 34, 1835–1842.

Yo, C., & Wilson, H. R. (1992). Perceived direction of moving two-dimensional patterns depends on duration, contrast and eccentricity. *Vision Research*, 32, 135–147.

Yuille, A. A. L., & Grzywacz, N. N. M. (1988). A computational theory for the perception of coherent visual motion. *Nature*, 333(6168), 71–74.

Appendix A: Formal analysis of stimulus ambiguity

Proof: The concentric dynamic Gabor array is consistent with multiple global motion solutions including a translation and rotation about some point (excluding the central point) along a line orthogonal to the specified translation through the center of the display.

We wish to show that the concentric Gabor array used in these experiments is consistent with several global motion patterns. To do this we define the local 2D motion at each position in the array for both translation and rotation about a point and show that

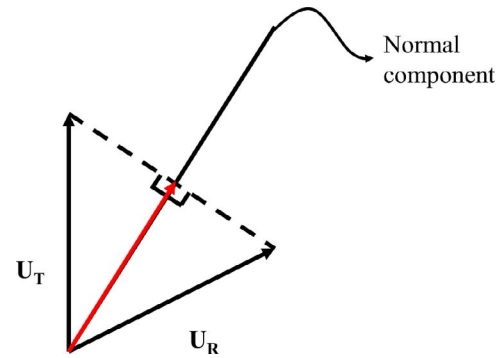


Figure A1. A drifting Gabor is simultaneously consistent with two 2D motion vectors, U_T and U_R (black arrows), if their projection onto the Gabor's normal component produces the same motion vector (red arrow).

when these vectors are projected onto the normal components of the dynamic Gabors, they produce the exact same set of vectors.

To simplify the mathematical description, we choose our coordinate system so that the concentric arrangement of 1D motion is centered on the origin. This means the 1D motion (i.e., normal component) at each point is parallel to the Gabor's position vector, $\mathbf{X} = (x_1, x_2)$.

We assume, without loss of generality, that the translation motion is upward, i.e., $U_T = (0, T)$. Then the 1D motion of each Gabor is given by projecting U_T onto \mathbf{X} :

$$C_T = \frac{U_T \cdot \mathbf{X}}{\mathbf{X} \cdot \mathbf{X}} \mathbf{X} = (0, T) \cdot (x_1, x_2) \times \frac{\mathbf{X}}{|\mathbf{X}|^2} \\ = T x_2 \times \frac{\mathbf{X}}{|\mathbf{X}|^2} \quad (1)$$

where \cdot denotes the dot product and \times denotes multiplication by a scalar. Now consider a rotation centered on some arbitrary point on the x axis, i.e., $\mathbf{P}_c = (x_c, 0)$. Then the underlying 2D motion at each point is $U_R = R(x_2, -(x_1 - x_c))$, where R is the angular momentum. Projecting this onto \mathbf{X} we can again find the 1D motion in the normal component direction that is consistent with this rotation.

$$C_R = \frac{U_R \cdot \mathbf{X}}{\mathbf{X} \cdot \mathbf{X}} \mathbf{X} \\ = R(x_2, -(x_1 - x_c)) \cdot (x_1, x_2) \times \frac{\mathbf{X}}{|\mathbf{X}|^2} \\ = R(x_1 x_2 - x_1 x_2 + x_c x_2) \times \frac{\mathbf{X}}{|\mathbf{X}|^2} \\ = R x_c x_2 \times \frac{\mathbf{X}}{|\mathbf{X}|^2} \quad (2)$$

Comparing Equations 1 and 2 we see that these will give the same 1D motions if $R x_c = T$. So for a fixed translation speed, T , and for every point on the x axis, $(x_c, 0)$ (except for the case where $x_c = 0$), there is a speed

of rotation, R , around that point such that the concentric Gabor array is entirely consistent, i.e., an infinite number of underlying global motions will produce the exact same local velocities in this Gabor array.

Appendix B: Analysis of the average speeds of global motions

Proof: The global translation solution is always slower than the average speed of any global rotation solution for our stimulus.

Taking the center of our array as the origin, then at any point (x_1, x_2) the local motion of a field rotating about some arbitrary point $(x_c, 0)$ is given by $\mathbf{U}_R = R(x_2, -(x_1 - x_c))$ and similarly the translation motion is given by $\mathbf{U}_T = (0, T)$, and, as we have already seen in Appendix A, $Rx_c = T$. Now if we take a circle of points, centered on the center of our array and of radius a , then $(x_1, x_2) = (a \cos \theta, a \sin \theta)$ for $\theta \in [0, 2\pi]$. The speed of the rotating field at these points can be found by,

$$\begin{aligned} |\mathbf{U}_R| &= \sqrt{R^2(x_2^2 + (x_1 - x_c)^2)} \\ &= \sqrt{R^2(a^2 \sin^2 \theta + a^2 \cos^2 \theta + x_c^2 - 2ax_c \cos \theta)} \\ &= R\sqrt{(a^2 + x_c^2 - 2ax_c \cos \theta)} = f(\theta) \end{aligned} \tag{3}$$

To find the average speed of all points on this circle we need to integrate $f(\theta)$ over $\theta \in [0, 2\pi]$ and divide by 2π . However, the integral of $f(\theta)$ has no closed form. But we note that the square root in Equation 3 refers to the positive root (speed is always positive) so

the whole is always positive. Now, if we first assume that $x_c \geq a$ then $R(x_c - a \cos \theta) \geq 0$ and,

$$\begin{aligned} (R(x_c - a \cos \theta))^2 &= R^2(x_c^2 + a^2 \cos^2 \theta - 2ax_c \cos \theta) \\ &\leq R^2(x_c^2 + a^2 - 2ax_c \cos \theta) \\ &= (R\sqrt{(x_c^2 + a^2 - 2ax_c \cos \theta)})^2 \\ &= (f(\theta))^2 \end{aligned} \tag{4}$$

so $(f(\theta))^2 \geq (R(x_c - a \cos \theta))^2$ and because they are both positive this implies that $f(\theta) \geq R(x_c - a \cos \theta)$. We can easily find the mean of the right hand side of this inequality to put a lower bound on the mean of $f(\theta)$, i.e.

$$\begin{aligned} \frac{1}{2\pi} \int_0^{2\pi} f(\theta) d\theta &\geq \frac{1}{2\pi} \int_0^{2\pi} R(x_c - a \cos \theta) d\theta \\ &= \frac{1}{2\pi} \int_0^{2\pi} Rx_c d\theta - \frac{1}{2\pi} \int_0^{2\pi} a \cos \theta d\theta \\ &= \frac{1}{2\pi} 2\pi Rx_c - 0 = Rx_c = T \end{aligned} \tag{5}$$

Now, in the alternate case we assume that $x_c < a$ then we can swap a and x_c in Equation 4, noting that now $R(a - x_c \cos \theta) > 0$, and similarly show that $f(\theta) \geq R(a - x_c \cos \theta)$, and the mean of this is $Ra > Rx_c = T$; so again the average speed of rotation is greater than translation. This is true for all values of x_c and for any circle centred on the centre of our array, so it is certainly true for our annular arrangement. For completeness we note that the inequality in Equation (4) becomes an equality (for all values of θ) if and only if $a = 0$, i.e., the singular point at the centre of the array.